

Quantum Lyapunov exponents

P. Falsaperla and G. Fonte

*Dipartimento di Fisica e Astronomia, Università di Catania, Corso Italia 57, I-95129 Catania, Italy
and Istituto Nazionale di Fisica Nucleare, Sezione di Catania, Corso Italia 57, I-95129 Catania, Italy*

Giovanni Salesi

*Facoltà di Ingegneria, Università Statale di Bergamo, I-24044 Dalmine (BG), Italy
and Istituto Nazionale di Fisica Nucleare, Sezione di Milano, I-20133 Milano, Italy*

(Dated: November 6, 2018)

We show that it is possible to associate univocally with each given solution of the time-dependent Schrödinger equation a particular phase flow (“quantum flow”) of a non-autonomous dynamical system. This fact allows us to introduce a definition of chaos in quantum dynamics (quantum chaos), which is based on the classical theory of chaos in dynamical systems. In such a way we can introduce quantities which may be appelled *quantum Lyapunov exponents*. Our approach applies to a non-relativistic quantum-mechanical system of n charged particles; in the present work numerical calculations are performed only for the hydrogen atom. In the computation of the trajectories we first neglect the spin contribution to chaos, then we consider the spin effects in quantum chaos. We show how the quantum Lyapunov exponents can be evaluated and give several numerical results which describe some properties found in the present approach. Although the system is very simple and the classical counterpart is regular, the most non-stationary solutions of the corresponding Schrödinger equation are *chaotic* according to our definition.

INTRODUCTION

Around the turn of the century, Poincaré pointed out a property which is typical of most mechanical systems. Although the evolution is deterministic, it shows an extreme sensitivity to initial conditions. Errors in these latter can grow up at an exponential rate, and thus in practice, long-time predictions become impossible and the evolution appears irregular and random. In the modern literature this phenomenon is called “deterministic chaos” or also “classical chaos”. [24] In the context of classical mechanics, it upsets the laplacian ideal of exact predictability, but, in the context of quantum mechanics, it rises even more profound problems. Indeed, in virtue of Bohr’s correspondence principle, one expects that quantum mechanics must include or imitate, in some way, classical chaos. The direct analogue of this in quantum mechanics should be a sort of exponential sensitivity to the initial conditions in the solutions of the time-dependent Schrödinger equation. The difficulty to put in evidence such a phenomenon is well known [1, 2] and the reason is obvious. In quantum mechanics, instead of individual trajectories, we have a field: the wave-function $\psi(\mathbf{r}, t)$, whose time-evolution is given by

$$\psi(\mathbf{r}, t) = \mathcal{U}(t, t_0)\psi(\mathbf{r}, t_0), \quad (1)$$

where $\mathcal{U}(t, t_0)$ is a unitary operator [3] on L^2 . Thus, according to L^2 -norm, two nearby initial wave-functions remain close as time evolves. Owing to this fact, which seems to rule out any possibility of a chaotic behaviour in quantum mechanics formally analogous to the classical one, the investigations on the subject have moved toward a different direction, that is in search of traces of classical chaos which persist in the quantum world. Although this research has obtained (see Ref. [1, 2] and references therein) interesting and far-reaching results, it looks less fundamental than the attempt of finding out a property of the quantum-mechanical time-evolution which is analogous to classical chaos. In the present paper, we show that such a property really exists. To put in evidence it, we give up, obviously, the too “rough” L^2 -norm to measure wave-function modifications and go to examine, so to say, “submicroscopical” details in the time-evolution (1). In short, these details are the “trajectories” $\mathbf{r} = \mathbf{r}(t)$ determined by the condition of being tangent at any point \mathbf{r} to the “velocity field” $\mathbf{V}(\mathbf{r}, t) = \mathbf{J}(\mathbf{r}, t)/\rho(\mathbf{r}, t)$ at time t and at point \mathbf{r} , where $\mathbf{J}(\mathbf{r}, t)$ and $\rho(\mathbf{r}, t)$ are, respectively, the probability density current and the probability density relative to the wave-function $\psi(\mathbf{r}, t)$. We shall see that the set of these trajectories, distributed with the probability density $\rho(\mathbf{r}, t)$, can be considered as a particular phase flow (quantum flow) of an usual non-autonomous dynamical system, univocally determined by the wave-function $\psi(\mathbf{r}, t)$ in (1). This latter fact permits us to introduce a definition of chaos for the time-evolution (1), founded only on the basic concepts of the theory of chaos in dynamical systems. We call such a definition of chaos *quantum chaos*. As we shall see, our characterization of chaos in quantum dynamics implies also a sort of exponential sensitivity to the initial conditions in the Schrödinger equation and thus, it is the direct analogue of classical chaos. Notice that the emergence of quantum chaos, by “unraveling” the quantal evolution (1) into “individual trajectories” is,

in a way, similar to the emergence of classical chaos in Hamiltonian systems, by “unraveling” the time-evolution of the phase space probability distribution $\rho(q, p, t)$ into individual particle trajectories. Indeed, since the equation (Liouville equation) satisfied by $\rho(q, p, t)$ is linear, slight modifications in the initial phase space probability distribution never lead [2] to exponential divergences of $\rho(q, p, t)$, although all or part of its “underlying” trajectories may be chaotic.

It should be observed that our approach is formally similar to the one recently proposed [4, 5, 6] within the framework of the de Broglie-Bohm causal interpretation of quantum mechanics (Bohmian mechanics), however it presents the following novelties:

- Our approach seems to be fuller.
- We do not make recourse to any new interpretation of quantum mechanics.
- We introduce suitable parameters (quantum Lyapunov exponents) to quantify quantum chaos.
- We show a calculation of these parameters in a system simple but realistic (hydrogen atom).
- We show intriguing relationships between quantum-mechanical quantities along a given trajectory and the Lyapunov exponents of this latter.

Although all the numerical results presented (Sec. 5) concern the hydrogen atom, our characterization of quantum chaos and the relative implications (Secs. 2-4) are discussed in the general setting of a quantum system of n charged particles.

THE QUANTUM FLOW

In this section we show how it is possible to associate univocally with a given solution $\psi(\mathbf{r}, t)$ of the initial value problem (IVP) for the Schrödinger equation a suitable phase flow of an usual non-autonomous dynamical system.

Let us consider a system of n particles with masses m_1, \dots, m_n and charges e_1, \dots, e_n . The corresponding Schrödinger equation writes

$$i\hbar \frac{\partial \psi(\mathbf{r}, t)}{\partial t} = \left[- \sum_{i=1}^n \frac{\hbar^2}{2m_i} \Delta_i + \sum_{i < j} \frac{e_i e_j}{|\mathbf{r}_i - \mathbf{r}_j|} \right] \psi(\mathbf{r}, t), \quad (2)$$

where $\mathbf{r} = (\mathbf{r}_1, \dots, \mathbf{r}_n)$, $\mathbf{r}_i \in \mathbb{R}^3$, $i = 1, 2, \dots, n$. Each wave-function

$$\psi(\mathbf{r}, t) = [\rho(\mathbf{r}, t)]^{1/2} e^{iS(\mathbf{r}, t)/\hbar} \quad (3)$$

satisfying Eq. (2) generates a probability density current

$$\mathbf{J}(\mathbf{r}, t) = (j_1(\mathbf{r}, t), \dots, j_n(\mathbf{r}, t)),$$

where

$$j_i(\mathbf{r}, t) := \frac{\rho(\mathbf{r}, t)}{m_i} [\nabla_i S(\mathbf{r}, t)], \quad i = 1, 2, \dots, n, \quad (4)$$

and hence a “velocity field”

$$\mathbf{V}(\mathbf{r}, t) = (v_1(\mathbf{r}, t), \dots, v_n(\mathbf{r}, t)), \quad (5)$$

where

$$v_i(\mathbf{r}, t) := \frac{j_i(\mathbf{r}, t)}{\rho(\mathbf{r}, t)}, \quad i = 1, 2, \dots, n. \quad (6)$$

The vector field (5) is not defined at any point $(\mathbf{r}, t) \in \mathbb{R}^{3n} \times \mathbb{R}_t$, where \mathbb{R}_t denotes the time axis. In general, we can say that it is defined on some set

$$\tilde{\mathcal{P}} = \mathbb{R}^{3n} \times \mathbb{R}_t / \mathcal{S},$$

where

$$\mathcal{S} = \{(\mathbf{r}, t) \in \mathbb{R}^{3n} \times \mathbb{R}_t : \text{ either } \psi(\mathbf{r}, t) = 0 \text{ (nodes)} \\ \text{ or } \psi(\mathbf{r}, t) \text{ is not differentiable}\}.$$

We call the set $\tilde{\mathcal{P}}$ *extended phase space*. We also need to consider the set

$$\mathcal{P} = \{\mathbf{r} \in \mathbb{R}^{3n} : (\mathbf{r}, t) \in \tilde{\mathcal{P}}, \text{ for some } t\}$$

and the set

$$\mathcal{P}(t) = \{\mathbf{r} \in \mathbb{R}^{3n} : (\mathbf{r}, t) \in \tilde{\mathcal{P}}, \text{ for } t \text{ fixed}\}.$$

We call the sets \mathcal{P} and $\mathcal{P}(t)$ *phase space* and *phase space at t*, respectively. Let us now introduce in the extended phase space $\tilde{\mathcal{P}}$ the “direction field” $(\mathbf{V}(\mathbf{r}, t), 1)$. It is easily seen [7, 8] that the curves in $\tilde{\mathcal{P}}$, which at any point (\mathbf{r}, t) have tangent directed as $(\mathbf{V}(\mathbf{r}, t), 1)$ in that point, can be described by the parametric equations $\mathbf{r} = \mathbf{r}(t), t = t$, where $\mathbf{r}(t)$ satisfies the equation

$$\dot{\mathbf{r}}(t) = \mathbf{V}(\mathbf{r}, t). \quad (7)$$

We name such curves *integral curves*. Notice that Eq. (7) defines what in the modern literature on chaos theory is referred to as *non-autonomous dynamical system*. For all we have said above, this system is determined univocally by the solution $\psi(\mathbf{r}, t)$ of a given IVP for the Schrödinger equation

$$\begin{cases} i\hbar\partial_t\psi(\mathbf{r}, t) = H\psi(\mathbf{r}, t) \\ \psi(\mathbf{r}, 0) =: \psi_0(\mathbf{r}), \quad \psi_0(\mathbf{r}) \in \mathcal{D}(H), \quad \|\psi_0(\mathbf{r})\| = 1, \end{cases} \quad (8)$$

where H is the Hamiltonian operator in (2) and $\mathcal{D}(H)$ its domain. In association with the IVP (8) we may also consider the following IVP

$$\begin{cases} \dot{\mathbf{r}}(t) = \mathbf{V}(\mathbf{r}, t) \\ \mathbf{r}(0) =: \mathbf{r}_0, \quad \mathbf{r}_0 \in \mathcal{P}(0). \end{cases} \quad (9)$$

The solution of (9), when represented in the extended phase space $\tilde{\mathcal{P}}$, coincides with the integral curve which goes through the point $(\mathbf{r}_0, 0)$. However, we prefer to think of the solution of (9) as the path (orbit) in the phase space \mathcal{P} followed, as time develops, by a point starting from \mathbf{r}_0 at $t = 0$. According to this representation, the solution of (9) will be called *trajectory*. Thus, the phase space \mathcal{P} is the region (which can also coincide with the whole \mathbb{R}^{3n}) accessible to our trajectories and the phase space at t , $\mathcal{P}(t)$, is the subregion of \mathcal{P} crossed by our trajectories at time t . [25] It should be observed that both the trajectory $\mathbf{r} = \mathbf{r}(t)$ and the corresponding orbit are tangent at any point \mathbf{r} to the velocity field $\mathbf{V}(\mathbf{r}, t)$ at time t and at point \mathbf{r} and that the orbit is the projection onto \mathcal{P} of the integral curve. Obviously, in the spirit of the usual interpretation of quantum mechanics, the trajectories of the IVP (9) do not correspond to an effective motion of quantum particles. However, this fact does not have any relevance at all in our characterization of chaos in quantum dynamics. Indeed, as we shall see, what is most important to this aim is that the trajectories of the IVP (9) are *formally analogous* to trajectories of real point particles. Another consideration about our trajectories is that they must exist uniquely and globally in time, i.e. for all $t \in \mathbb{R}_t$. This property is, in fact, of basic importance to apply the theory of chaos in dynamical systems. Thus, we turn now our attention to it. First of all, we note that a prerequisite of this property is that the velocity field (5) exists uniquely and globally in time, i.e. the IVP (8) admits an unique and global solution. In order that it be true, all is required is [3] the self-adjointness of H , property which in our case is valid [3]. Consider now the main question: does the IVP (9) determined by (8) admit an unique and global solution? This question turns out to be more difficult, because the solution of (9) may run into catastrophic events, such as reaching in finite time a point of the set \mathcal{S} (the singularities of the velocity field). The question, which is also of basic importance in Bohmian mechanics, has been investigated recently [9]. The findings of the paper [9] are that, for a large class of potentials (including the Coulomb potential in (2)) and under certain hypotheses (see [9] for details), the IVP (9) admits an unique and global solution. This basic property will be assumed throughout the present paper. Now, in order to make more precise the definition of trajectory as well as the definition of quantum flow to be given below, we find it convenient to introduce the following mappings:

a) $\Phi(\cdot, t_1, \mathbf{r}_1) : \mathbb{R}_t \rightarrow \mathcal{P}$. This mapping represents the trajectory of the IVP (9), which goes through the point \mathbf{r}_1 at time t_1 . Thus $\Phi(t, t_1, \mathbf{r}_1) = \mathbf{r}(t)$ represents the coordinate \mathbf{r} at time t of the point pursuing this trajectory.

b) $\Phi(\cdot, t_1, \cdot) : \mathbb{R}_t \times \mathcal{P}(t_1) \rightarrow \mathcal{P}$. In the theory of dynamical systems, this mapping is called *phase flow*. In our picture, it represents the set of all trajectories of the IVP(9), passing through $\mathcal{P}(t_1)$ at time t_1 .

c) $\Phi(t, t_1, \cdot) : \mathcal{P}(t_1) \rightarrow \mathcal{P}(t)$. We call this mapping *phase flow at t*.

The existence of these mappings is due [7, 10] to the assumption that the IVP (9) admits an unique and global solution. This assumption implies also [7, 10] the following properties:

d) For $t_1, t_2 \in \mathbb{R}_t$ fixed, the mapping $\Phi(t_2, t_1, \cdot) : \mathcal{P}(t_1) \rightarrow \mathcal{P}(t_2)$ is one-to-one, differentiable and with inverse differentiable (diffeomorphism).

e) $\Phi(t, t, \cdot) = I$ (identity).

f) $\Phi(t, t_2, \Phi(t_2, t_1, \mathbf{r}_1)) = \Phi(t, t_1, \mathbf{r}_1)$ (chain rule) [26]

Now, let us introduce on $\mathcal{P}(0)$ a statistical ensemble \mathcal{E} of initial conditions (points), distributed according to the probability density $\tilde{\rho}_0(\mathbf{r}(0)) = \psi_0^*(\mathbf{r}(0))\psi_0(\mathbf{r}(0)) = \rho_0(\mathbf{r}(0))$, where $\psi_0(\mathbf{r})$ is the wave-function appearing in the IVP (8), and let us consider the time-evolution of these points according to the IVP (9), i.e. the phase flow $\Phi(\cdot, \cdot)$ defined on $\mathbb{R}_t \times \mathcal{E}$. We call this special realization of the phase flow *quantum flow* (QF). Thus from one hand, the QF is formally similar to the phase flow of an ordinary dynamical system, on the other hand it has characteristic peculiarities. In fact, the velocity field $\mathbf{V}(\mathbf{r}, t)$ in (9) depends on a specific solution of the IVP (8) and the initial conditions are distributed with a probability density, which is not uniform as in the phase flow of dynamical systems, but is given by $\rho_0(\mathbf{r}(0))$. The fact that to each given solution $\psi(\mathbf{r}, t)$ of (8) there corresponds an unique dynamical system (7) and hence an unique QF, gives us the opportunity of defining a chaotic behaviour in quantum dynamics. Indeed, we may say that the given $\psi(\mathbf{r}, t)$ is chaotic when the corresponding QF presents trajectories which are chaotic, according to the usual definition of classical chaos. We call this characterization of chaos in quantum dynamics *quantum chaos*.

As we shall show in Sec. 5, our definition of quantum chaos implies also a kind of extreme sensitivity to initial conditions, in the sense that a tiny modification in L^2 -norm in the initial condition $\psi(\mathbf{r}, 0)$ in (8) gives rise to a dramatic modification in the QF pattern: each chaotic trajectory turns into another diverging exponentially from it. Strictly speaking, the definition of quantum chaos given as above is not fully rigorous and does not put in evidence the role of the ensemble \mathcal{E} . A rigorous and satisfactory definition of quantum chaos as well as a precise measure of it are postponed until Sec. 4, because first we need to describe some properties of the QF and also to recall the methods to quantify classical chaos.

SOME PROPERTIES OF THE QUANTUM FLOW

The properties of the QF are essentially those of an ordinary phase flow. However, due to peculiarity of the QF, some of them show themselves under new light and imply intriguing connections with quantum mechanical properties. Thus, besides mentioning the main properties of the QF, we dwell particularly upon these new aspects, giving also some proof, when this turns out to be necessary to make the paper clear and self-contained [27].

Property 1. Denoting by $\tilde{\rho}(\mathbf{r}(t), t)$ the probability density of points $\mathbf{r}(t)$ in the ensemble \mathcal{E} on $\mathcal{P}(t)$, the assumption, in the previous section, that the density of points in \mathcal{E} at $t = 0$ on $\mathcal{P}(0)$ is $\tilde{\rho}_0(\mathbf{r}(0)) = \rho_0(\mathbf{r}(0))$, implies [4, 9] $\tilde{\rho}(\mathbf{r}(t), t) = \psi^*(\mathbf{r}(t), t)\psi(\mathbf{r}(t), t) = \rho(\mathbf{r}(t), t)$, $\forall t > 0$ and $\forall \mathbf{r}(t) \in \mathcal{P}(t)$.

Property 2. Let \mathbf{r}_0 be a given point of $\mathcal{P}(0)$ and $d\mathbf{r}_0$ be the volume element around this point [28]. Let $\mathbf{r}(t)$ and $d\mathbf{r}(t)$ be the corresponding quantity transformed by the QF at $t > 0$, i.e. $\mathbf{r}(t) = \Phi(t, \mathbf{r}_0)$, $d\mathbf{r}(t) = \Phi(t, d\mathbf{r}_0)$. Then, the probability measure $\rho(\mathbf{r}(t), t) d\mathbf{r}(t)$ is invariant under the QF, i.e.

$$\rho_0(\mathbf{r}_0) d\mathbf{r}_0 = \rho(\mathbf{r}(t), t) d\mathbf{r}(t), \quad \forall t > 0. \quad (10)$$

Proof. Think of the QF at t (cf. points c) and d) in Sec. 2) as the coordinate transformation

$$\Phi(t, \mathbf{r}(0)) = \mathbf{r}(t) \quad (11)$$

from $\mathcal{P}(0)$ to $\mathcal{P}(t)$, $t > 0$. We have

$$d\mathbf{r}(t) = J(t, \mathbf{r}_0) d\mathbf{r}_0, \quad (12)$$

where $J(t, \mathbf{r}_0)$ denotes the Jacobian at \mathbf{r}_0 [29] of the transformation (11). This Jacobian satisfies [11] the equation

$$J = \left(\sum_{i=1}^n \nabla_i \cdot \mathbf{v}_i \right) J, \quad (13)$$

where the quantities \mathbf{v}_i are given by (6). Integrate (13) with the initial condition $J(0, \mathbf{r}_0) = I$, and integrate the continuity equation for ρ in the Lagrangian form, i.e.,

$$\frac{d\rho}{dt} + \rho \left(\sum_{i=1}^n \nabla_i \cdot \mathbf{v}_i \right) = 0, \quad (14)$$

with the initial condition $\rho_0(\mathbf{r}_0)$. We find

$$\rho(\mathbf{r}(t), t) J(t, \mathbf{r}_0) = \rho_0(\mathbf{r}_0), \quad \forall t > 0,$$

which, in virtue of (12), yields the relationship (10). \square

Property 3. *The growth rate under the QF of the size of the volume element $d\mathbf{r}(t)$ around the point $\mathbf{r}(t)$ is given by*

$$\frac{d d\mathbf{r}(t)}{dt} = d\mathbf{r}(t) \left(\sum_{i=1}^n \nabla_i \cdot \mathbf{v}_i(\mathbf{r}(t), t) \right), \quad \forall t > 0. \quad (15)$$

The proof is an easy consequence of Property 2 and of (14). The integration of Eq. (15) over a finite volume $\mathcal{V}(t) \subset \mathcal{P}(t)$ yields

$$\frac{d\mathcal{V}(t)}{dt} = \int_{\mathcal{V}(t)} \left(\sum_{i=1}^n \nabla_i \cdot \mathbf{v}_i(\mathbf{r}(t), t) \right) d\mathbf{r}(t).$$

Since (see Eqs. (3,4,6))

$$\sum_{i=1}^n \nabla_i \cdot \mathbf{v}_i(\mathbf{r}(t), t) = \sum_{i=1}^n \frac{1}{m_i} (\Delta_i S(\mathbf{r}(t), t)),$$

we find that in a given region $\Omega \subset \tilde{\mathcal{P}}$, the QF is *conservative* or *nonconservative*, according to whether the value of $\sum_{i=1}^n \frac{1}{m_i} (\Delta_i S(\mathbf{r}(t), t))$ in Ω is equal to zero or different from zero, respectively.

We have to recall now the basic elements to define and quantify chaos in dynamical systems, i.e. the definition and the main properties of the Lyapunov exponents (LEs) of a given trajectory. We do that going in some details, because these are necessary to put in evidence the interesting connections mentioned at the beginning of this section as well as to explain part of the numerical results shown in Sec. 5.

According to Refs. [12, 13], the LEs of the trajectory $\Phi(\cdot, \mathbf{r}_0)$ starting from \mathbf{r}_0 at $t = 0$ and belonging to our QF, are defined by the following limit

$$\lambda(\mathbf{r}_0, \xi_0) := \lim_{t \rightarrow +\infty} \frac{1}{t} \ln \|U_{\mathbf{r}_0}(t) \xi_0\|, \quad (16)$$

as function of ξ_0 , where $\|\cdot\|$ is the Euclidean norm, ξ_0 is an arbitrary starting vector of \mathbb{R}^{3n} , $\|\xi_0\| = 1$, and $U_{\mathbf{r}_0}(t)$ is an $3n \times 3n$ invertible matrix (flow matrix). This matrix is the solution of the IVP

$$\begin{cases} \dot{U}_{\mathbf{r}_0}(t) = \left\{ \frac{\partial \mathbf{v}_i}{\partial \mathbf{r}_j} \Big|_{\Phi(\cdot, \mathbf{r}_0)} \right\}_{i,j=1}^n U_{\mathbf{r}_0}(t) \\ U_{\mathbf{r}_0}(0) = I, \end{cases} \quad (17)$$

obtained by linearization of (9). Rigorous results on the existence of the limit (16) and on the properties of the corresponding LEs can be found in Refs. [12, 13] and references therein. It is not easy to show (it would be also beyond the scope of the present paper) that the findings in [12, 13], proved under suitable hypotheses, can be taken over to the dynamical system (7). However, on the basis of a strong numerical evidence found by us in the case $3n = 3$, it seems reasonable to extend to (7) the validity of what follows:

i) Depending on the choice of ξ_0 , the limit (16) takes on $3n$ (not necessarily distinct) values:

$$\lambda_1(\mathbf{r}_0) \geq \lambda_2(\mathbf{r}_0) \geq \dots \geq \lambda_{3n}(\mathbf{r}_0).$$

ii) If ξ_0 is chosen arbitrarily, the value of the limit (16) is $\lambda_1(\mathbf{r}_0)$.

iii) Consider the symmetric and positive matrix

$$W_{\mathbf{r}_0}(t) := \left(\tilde{U}_{\mathbf{r}_0}(t) U_{\mathbf{r}_0}(t) \right)^{1/2t}, \quad (18)$$

where \tilde{U} denotes the transpose of U . Denote by $\mu_1(t, \mathbf{r}_0) \geq \dots \geq \mu_{3n}(t, \mathbf{r}_0)$ its eigenvalues. Let

$$\lambda_i(t, \mathbf{r}_0) := \ln \mu_i(t, \mathbf{r}_0), \quad i = 1, \dots, 3n. \quad (19)$$

Then,

$$\lim_{t \rightarrow +\infty} \lambda_i(t, \mathbf{r}_0) = \lambda_i(\mathbf{r}_0). \quad \square$$

The meaning of the LEs is put well in evidence by the following geometric argument. Consider the singular value decomposition [14] of the matrix $U_{\mathbf{r}_0}(t)$, i.e.

$$U_{\mathbf{r}_0}(t) L_{\mathbf{r}_0}(t) = G_{\mathbf{r}_0}(t) F_{\mathbf{r}_0}(t), \quad t > 0, \quad (20)$$

where L and G are orthogonal matrices and F is a diagonal matrix with elements $\sigma_1(t, \mathbf{r}_0) \geq \sigma_2(t, \mathbf{r}_0) \geq \dots \geq \sigma_{3n}(t, \mathbf{r}_0) > 0$. Take account of the fact that (20) implies

$$\tilde{L}_{\mathbf{r}_0}(t) W_{\mathbf{r}_0}(t)^{2t} L_{\mathbf{r}_0}(t) = F_{\mathbf{r}_0}^2(t),$$

so that the columns of L are the orthonormal eigenvectors $\mathbf{e}_1(t, \mathbf{r}_0), \dots, \mathbf{e}_{3n}(t, \mathbf{r}_0)$ of $W_{\mathbf{r}_0}(t)$ and

$$\sigma_i(t, \mathbf{r}_0) = \exp[\lambda_i(t, \mathbf{r}_0)t], \quad i = 1, \dots, 3n. \quad (21)$$

Then,

$$U_{\mathbf{r}_0}(t) \mathbf{e}_i(t, \mathbf{r}_0) = \exp[\lambda_i(t, \mathbf{r}_0)t] \mathbf{e}'_i(t, \mathbf{r}_0), \quad i = 1, \dots, 3n, \quad (22)$$

where $\mathbf{e}'_i(t, \mathbf{r}_0)$ are the columns of G . Let now $d\mathbf{r}_0$ be an infinitesimal parallelepiped, with axes $\varepsilon_i \mathbf{e}_i(t, \mathbf{r}_0)$, $i = 1, \dots, 3n$, which at $t = 0$ is placed at \mathbf{r}_0 . Since the ε_i are infinitesimal,

$$U_{\mathbf{r}_0}(t) \varepsilon_i \mathbf{e}_i(t, \mathbf{r}_0) \simeq \Phi(t, \mathbf{r}_0 + \varepsilon_i \mathbf{e}_i(t, \mathbf{r}_0)) - \Phi(t, \mathbf{r}_0) , \\ i = 1, \dots, 3n ,$$

and thus, in virtue of (22), the phase flow at $t > 0$ transforms $d\mathbf{r}_0$ into another infinitesimal parallelepiped $d\mathbf{r}(t)$, which presents a different orientation in \mathbb{R}^{3n} and the i th axis, $i = 1, \dots, 3n$, grown or shrunk according as the corresponding $\lambda_i(t, \mathbf{r}_0)$ is positive or negative, respectively. The value of $\lambda_i(t, \mathbf{r}_0)$ gives the rate at time t of the exponential growing or shrinking of this axis. The meaning of $\lambda_i(\mathbf{r}_0)$, $i = 1, \dots, 3n$, is then obtained accordingly in the limit $t \rightarrow +\infty$ [30]. We can now prove the following property:

Property 4. *Let $d\mathbf{r}_0$ and $d\mathbf{r}(t)$ be volume elements the same as in Property 2. Suppose $d\mathbf{r}_0$ is a parallelepiped. Then,*

$$d\mathbf{r}(t) = d\mathbf{r}_0 \exp \left[\sum_{i=1}^{3n} \lambda_i(t, \mathbf{r}_0) t \right], \quad \forall t > 0. \quad (23)$$

Proof. In virtue of (22), each axis

$$d\xi_i = \varepsilon_1^i \mathbf{e}_1(t, \mathbf{r}_0) + \dots + \varepsilon_{3n}^i \mathbf{e}_{3n}(t, \mathbf{r}_0), \quad i = 1, \dots, 3n,$$

of $d\mathbf{r}_0$ is transformed according to

$$U_{\mathbf{r}_0}(t)d\boldsymbol{\xi}_i = d\boldsymbol{\xi}'_i = \varepsilon_1^i \exp[\lambda_1(t, \mathbf{r}_0)t] \mathbf{e}'_1(t, \mathbf{r}_0) + \dots + \varepsilon_{3n}^i \exp[\lambda_{3n}(t, \mathbf{r}_0)t] \mathbf{e}'_{3n}(t, \mathbf{r}_0).$$

Taking account of this fact and recalling that the $3n$ -dimensional volume spanned by $3n$ linearly independent vectors arranged in an $3n \times 3n$ matrix A is $|\det(A)|$, the proof is completed by a straightforward calculation. \square

The relationship (23) entails two more properties.

Property 5.

$$\rho(\mathbf{r}(t), t) = \rho_0(\mathbf{r}_0) \exp \left[- \sum_{i=1}^{3n} \lambda_i(t, \mathbf{r}_0)t \right], \quad \forall t > 0, \quad (24)$$

where the points $\mathbf{r}(t)$ and \mathbf{r}_0 are the same as in Property 2 and $\rho(\mathbf{r}(t), t) = \psi^*(\mathbf{r}(t), t)\psi(\mathbf{r}(t), t)$.

Property 6.

$$\sum_{i=1}^n \frac{1}{m_i} (\Delta_i S(\mathbf{r}(t), t)) = \sum_{i=1}^{3n} [\lambda_i(t, \mathbf{r}_0) + \dot{\lambda}_i(t, \mathbf{r}_0)t] , \quad \forall t > 0 , \quad (25)$$

where S is the phase of $\psi(\mathbf{r}, t)$ in the polar form (3) and the points $\mathbf{r}_0, \mathbf{r}(t)$ are the same as in Property 2.

The proof of (24) is a straightforward consequence of (23) and of Property 2. To prove (25), it is enough to differentiate with respect to t Eq. (23) and then to compare the result with (15) and to recall (4) and (6). These two latter properties seems to us somewhat intriguing, for the following reason. The quantities $\lambda_i(t, \mathbf{r}_0)$ are functions of t and hence of the point $\mathbf{r}(t) = \Phi(t, \mathbf{r}_0)$. Therefore, they may be looked upon as “classical dynamical variables” of the point pursuing the the trajectory $\Phi(\cdot, \mathbf{r}_0)$. In virtue of the relationships (24) and (25), these variables are strictly correlated to the time-evolution of $\psi(\mathbf{r}, t)$ along the given trajectory.

QUANTUM LYAPUNOV EXPONENTS

In this section, we give the precise definition of chaotic solution for the IVP (8) and at the same time we give the tool to measure the corresponding degree of quantum chaos. We get this tool by considering a properly weighted average of the LEs of all trajectories in the associated QF.

Definition 1. Let $\psi(\mathbf{r}, t)$ be the solution of the IVP (8). Recall that $\rho_0(\mathbf{r}(0))$ is the corresponding probability density of points in our statistical ensemble \mathcal{E} at $t = 0$. Then, the quantities

$$\Lambda_i(0) := \int_{\mathcal{P}(0)} \lambda_i(\mathbf{r}(0)) \rho_0(\mathbf{r}(0)) d\mathbf{r}(0), \quad i = 1, 2, \dots, 3n, \quad (26)$$

where $\lambda_i(\mathbf{r}(0))$ is the i th LE of the trajectory of (9) starting from $\mathbf{r}(0)$ at $t = 0$, are called “quantum Lyapunov exponents” (QLE) of the given $\psi(\mathbf{r}, t)$. For the sake of simplicity hereafter we suppose the usual normalization $N \equiv \int_{\mathcal{P}(0)} \rho_0(\mathbf{r}(0)) d\mathbf{r}(0) = 1$; if $N \neq 1$, we must divide by N the r.h.s. of eq. (26).

Property 7. The QLEs are invariant under the QF, i.e.,

$$\Lambda_i(0) = \Lambda_i(t) := \int_{\mathcal{P}(t)} \lambda_i(\mathbf{r}(t), t) \rho(\mathbf{r}(t), t) d\mathbf{r}(t) , \quad i = 1, 2, \dots, 3n, \quad \forall t > 0 ,$$

where $\mathbf{r}(t) = \Phi(t, \mathbf{r}(0))$ and $\lambda_i(\mathbf{r}(t), t)$ is the LE of the trajectory of (9) starting from $\mathbf{r}(t)$ at t .

Proof. As in the proof of Property 2, think of the QF at t as the coordinate transformation $\Phi(t, \mathbf{r}(0)) = \mathbf{r}(t)$, from $\mathcal{P}(0)$ to $\mathcal{P}(t)$. We find

$$\begin{aligned}\Lambda_i(t) &:= \int_{\mathcal{P}(t)} \lambda_i((\mathbf{r}(t), t)) \rho((\mathbf{r}(t), t)) d\mathbf{r}(t) \\ &= \int_{\mathcal{P}(0)} \lambda_i(\Phi(t, \mathbf{r}(0)), t) \rho_0(\mathbf{r}(0)) d\mathbf{r}(0) \\ &= \int_{\mathcal{P}(0)} \lambda_i(\mathbf{r}(0)) \rho_0(\mathbf{r}(0)) d\mathbf{r}(0) \\ &=: \Lambda_i(0), \quad i = 1, 2, \dots, 3n, \quad \forall t > 0,\end{aligned}$$

where we have employed (10) and the property $\lambda_i(\Phi(t, \mathbf{r}(0)), t) = \lambda_i(\mathbf{r}(0))$ which follows from the very definition of LE. \square

According to the above property, the QLEs are parameters whose values are univocally correlated to peculiar features of a given quantal evolution, i.e. the chaotic behaviour of the trajectories in the associated QF. Therefore, in correspondence with the definition of classical chaos, we can introduce the following definition:

Definition 2. *A given solution of the IVP (8) is called “chaotic” if the leading QLE Λ_1 [31] is positive. The value of Λ_1 is assumed as a measure of the corresponding quantum chaos.*

Notice that employing only Λ_1 in the definition above corresponds to the fact that the quantity of main interest, to quantify chaos in a dynamical system, is the leading LE. Another quantity is the so-called KS entropy [2, 15] which requires all the positive LEs. In principle, an analogous parameter employing all the positive QLEs, could be introduced also here, but we do not find it necessary to discuss this point further in the present paper.

NUMERICAL RESULTS

Since the leading QLE is a precise indicator of our characterization of quantum chaos, most of the present section is devoted to discuss in some detail, through a numerical example, how it is possible to calculate it. We also show numerical results to illustrate some properties of the QF and the complex variety of the underlying trajectories. As is evident from the definition (26), the computation of Λ_1 is, in general, very difficult. Indeed, once assigned a given solution [32] $\psi(\mathbf{r}, t)$ of the IVP (8), this calculation requires what follows:

- 1) Numerical integration of the IVP (9), associated with the given wave-packet $\psi(\mathbf{r}, t)$.
- 2) Calculation of the LE $\lambda_1(\mathbf{r}(0))$ for all trajectories in the QF relative to $\psi(\mathbf{r}, t)$.
- 3) Evaluation of the integral (26), in the case $i = 1$.

As we shall see, each point above presents peculiar numerical problems. The numerical example shown below is relative to the calculation of Λ_1 , in the case of the wave-packet

$$\begin{aligned}\psi(\mathbf{r}, t) &= \frac{1}{\sqrt{3}} \left(\varphi_{100}(\mathbf{r}) e^{\frac{i}{2}t} + \varphi_{200}(\mathbf{r}) e^{\frac{i}{8}t} + \varphi_{211}(\mathbf{r}) e^{\frac{i}{8}t} \right) \\ &= \rho^{1/2}(\mathbf{r}, t) e^{iS(\mathbf{r}, t)},\end{aligned}\tag{27}$$

where $\varphi_{nlm}(\mathbf{r})$ denote eigenfunctions of the hydrogen atom [33]. The chosen wave-function is the most simple superposition of the hydrogen atom eigenstates entailing, as we are going to show, the presence of quantum chaos and non-vanishing QLEs. As concerns point 1), we employ an adaptive fourth-order Runge-Kutta method, evaluating numerically the velocity field $\mathbf{v}(\mathbf{r}, t) = \nabla S(\mathbf{r}, t)$ appearing in (9). We find that a considerable portion of the trajectories are chaotic, i.e. $\lambda_1(\mathbf{r}(0)) > 0$. This fact implies the well known difficulty [16] about the integration of chaotic systems: numerical errors propagate exponentially and the trajectories after a certain time, depending on the accuracy of the algorithm employed, become meaningless. This phenomenon is amplified if, as in our case (see below), there is no attractor. However, rather than in trajectories, we are interested in the corresponding LEs, and these latter (see Fig. 1) are stable to within 10%.

As concerns point 2), we should evaluate only $\lambda_1(\mathbf{r}(0))$, the largest of the three LEs which appear in our example. However, since we want to check the relationship (24) and also for reasons (see below) of numerical control, actually, we calculate all three LEs. It is well known [16, 17] that, contrarily to the evaluation of the only leading LE, the calculation of all of them present numerical difficulties and special techniques are called for. In the present paper we have employed the algorithm introduced in Ref. [17] (BGGS algorithm) and described also in Ref. [16].

This algorithm is based on formula (16), when one is interested only in the evaluation of the leading LE, otherwise it employs the more general formula

$$\begin{aligned} \lambda_1(\mathbf{r}_0) + \dots + \lambda_p(\mathbf{r}_0) &= \\ \lim_{t \rightarrow +\infty} \frac{1}{t} \ln \text{Vol}^p \{U_{\mathbf{r}_0}(t)\xi_1 \dots U_{\mathbf{r}_0}(t)\xi_p\}, \\ 1 \leq p \leq 3n, \end{aligned} \quad (28)$$

where ξ_1, \dots, ξ_p are orthonormalized starting vectors arbitrarily chosen, $\text{Vol}^p \{\cdot\}$ denotes the volume of the parallelepiped defined by the vectors $U_{\mathbf{r}_0}(t)\xi_1, \dots, U_{\mathbf{r}_0}(t)\xi_p$ and \mathbf{r}_0 is the specific point from which the trajectory starts at $t = 0$. The peculiarity of the BGGS algorithm is that of making use of successive orthonormalization procedures in order to avoid well-known [16, 17] problems of overflow and of “alignment” of the starting vectors. With this trick, the BGGS algorithm turns out to be very effective and preferable to the evaluation of the LEs directly as logarithms of the eigenvalues of the matrix (18). Notice that the BGGS algorithm yields, in practice, approximations $\lambda_i(t, \mathbf{r}_0)$, $i = 1, \dots, 3n$, as functions of t for the LEs. In comparison with the analogous quantities (19), the BGGS approximations are, as we said, more reliable numerically. On the other hand, contrarily to (19), they depend on the starting vectors ξ_1, \dots, ξ_p , and thus, strictly speaking, they cannot be considered as the “dynamical variables” which enter into the relationships (23)-(25). However, in spite of the fact that the quantities (19) and the BGGS approximations coincide only in the limit $t \rightarrow +\infty$, the respective sums of all them coincide at each t . This latter property may be seen comparing Eq. (23) with the analogous one obtained by truncating at t Eq. (28) in the case $p = 3n$. In virtue of this coincidence, we shall employ the quantities $\lambda_i(t, \mathbf{r}_0)$ obtained by the BGGS algorithm to check relationship (24). The numerical difficulty of point 2) is that the wave-packet (27), notwithstanding its simplicity, gives rise to a complex scenario of trajectories. In fact, we find trajectories whose behaviour passes, through all the intermediate degrees, from the regular one to the chaotic one including also the so-called “intermittency” [2]. In this latter case, the trajectory switches back and forth between two qualitatively different behaviours, which in our case are the mildly chaotic one and the chaotic one. To put in evidence these different regimes, we show a typical regular trajectory (Fig. 2a), a typical “intermittent” chaotic trajectory (Fig. 2b) and a typical chaotic trajectory (Fig. 2c), and for each of them, together with the LE $\lambda_1(t, \mathbf{r}_0)$ [34] as function of t , we display the quantities

$$\lambda^{(k)} := \frac{1}{\Delta t} \ln \frac{\|U_{\mathbf{r}(t_k)}(t_{k+1}, t_k)\xi(t_k)\|}{\|\xi(t_k)\|}, \quad (29)$$

where $k = 0, 1, 2, \dots$, $\mathbf{r}(t_k) = \Phi(t_k, \mathbf{r}_0)$, $t_k = k \Delta t$ and $\xi(t_{k+1}) = U_{\mathbf{r}(t_k)}(t_{k+1}, t_k)\xi(t_k)$. The symbol $U_{\mathbf{r}(t_k)}(t_{k+1}, t_k)$ denotes the flow matrix solution of the IVP (17) with initial condition at $t = t_k$, $U_{\mathbf{r}(t_k)}(t_k, t_k) = I$. In other words, the $\lambda^{(k)}$ measure the rate of the exponential divergence or convergence, in the time interval (t_{k+1}, t_k) , of the two trajectories: $\Phi(\cdot, \mathbf{r}_0)$ (the fiducial trajectory) and $\Phi(\cdot, \mathbf{r}_0 + \varepsilon \xi_0)$, where ε is infinitesimal and ξ_0 is an arbitrary starting vector, $\|\xi_0\| = 1$. Furthermore, recalling the chain rule for the flow matrix (cf. point f) in Sec. 2), the definition (16) and point ii) in Sec. 3, we have

$$\lambda_1(t_N, \mathbf{r}_0) := \frac{1}{t_N} \ln \|U_{\mathbf{r}_0}(t_N)\xi_0\| = \frac{1}{N} \sum_{k=0}^{N-1} \lambda^{(k)}.$$

Strictly speaking, $\lambda_1(t_N, \mathbf{r}_0)$ shows a dependence on ξ_0 , which disappears in the limit $t \rightarrow +\infty$. Here, we do not find it necessary to investigate such a dependence, because in our case the LEs present a relative error of order 10%. The above mentioned complex scenario of trajectories has forced us to find out a numerical device (see below) capable of giving a reliable estimation of

$$\lambda_1(\mathbf{r}(0)) = \lim_{t \rightarrow +\infty} \lambda_1(t, \mathbf{r}(0)), \quad (30)$$

over the whole range of the chaotic behaviour. The point 3) in our example reduces to the evaluation of

$$\Lambda_1 = \int_{\mathcal{R}} \lambda_1(\mathbf{r}(0)) \rho_0(\mathbf{r}(0)) d\mathbf{r}(0), \quad (31)$$

where $\rho_0(\mathbf{r}(0))$ is the probability density in (27) at $t = 0$, $\mathbf{r}(0)$ varies on $\mathcal{R} \subset \mathcal{P}(0)$ and $\mathcal{R} = \{(x, y, z) : -9 < x < 9, -6 < y < 6, -8 < z < 8\}$ is a region such that the density $\rho_0(\mathbf{r}(0))$ is negligible outside. The numerical difficulty here is that the values of $\lambda_1(\mathbf{r}(0))$ are given, as we said, with a relative error of order 10%. For this reason, we have found it convenient to employ an adaptive Monte-Carlo method and to perform four integration runs with different accuracy parameters, [35] to see how much the errors over $\lambda_1(\mathbf{r}(0))$ affect the value of Λ_1 .

We pass now to describe how the actual evaluation of (31) is carried out. Chosen an initial condition $\mathbf{r}(0) \in \mathcal{R}$ by the Monte-Carlo routine, the integration of the IVP (9) and the BGGS algorithm start in simultaneously. After a time, say t_1 , large enough, we apply the numerical device previously mentioned to estimate the limit (30). Actually, this numerical device consists in two different convergence criteria. The first one is conceived to recognize regular trajectories and it is as follows. We divide the interval $I_1 = [0.4t_1, t_1]$ in five sub-intervals of equal lenght and compute a linear least squares approximation (LLSA) to $\lambda_1(t, \mathbf{r}(0))$ in each sub-interval. [36] If all the LLSAs are decreasing and the minimum of $\lambda_1(t, \mathbf{r}(0))$ on I_1 is smaller than a fixed threshold, [37] the corresponding trajectory is considered regular and its LE $\lambda_1(\mathbf{r}(0))$ in (30) is estimated at zero (Fig. 3). As concerns the second convergence criterion, conceived for chaotic trajectories, we compute a LLSA of the function $\lambda_1(t, \mathbf{r}(0))t$ on I_1 . If the root-mean-square-error in the LLSA is sufficiently small, the angular coefficient of the fitting straight line is assumed as value of $\lambda_1(\mathbf{r}(0))$ (Fig. 4). The integration of the IVP (9) and the BGGS algorithm stop, if one of the two convergence criteria is satisfied, otherwise they go on up to a certain time $t_2 > t_1$ and the two criteria are again applied on the new interval $[0.4t_2, t_2]$, and so on, until one of the two criteria is met. Then the procedure starts again with a new initial condition.

In order to evaluate the QLE (31) with a relative accuracy of 10%, the Monte-Carlo routine has employed about 1700 initial conditions and the corresponding CPU-time in a double-precision calculation on a workstation, has been about 60 hours. As we said, we have performed four such runs, varying the accuracy parameters, and the correspondent values found for Λ_1 are the following: $9.048 \cdot 10^{-3}$, $9.326 \cdot 10^{-3}$, $8.465 \cdot 10^{-3}$, $9.048 \cdot 10^{-3}$.

Notwithstanding the scenario of the trajectories pertaining to the wave-packet (27) is complex, we have found that our integration domain \mathcal{R} may be subdivided into three sufficiently disjoint regions, according to the $\lambda_1(\mathbf{r}(0))$ values. These three regions (Fig. 5) are: the regular one ($\lambda_1(\mathbf{r}(0)) = 0$), the mildly chaotic one ($0 < \lambda_1(\mathbf{r}(0)) < 10^{-2}$) and the chaotic one ($\lambda_1(\mathbf{r}(0)) \geq 10^{-2}$). On the basis of the values found for Λ_1 and considering also that the most chaotic trajectories have, in our units, LEs of order 0.04, we can say that the wave-packet (27) presents a good degree of quantum chaos. Although we have investigated in detail only the wave-packet (27), we have the numerical evidence, according to what observed in Ref. [5] for a different system, that there are chaotic trajectories in the QFs corresponding to most wave-packets relative to the hydrogen atom. Thus, even if the classical counterpart of the hydrogen atom is not chaotic, our characterization of quantum chaos seems to spread through the corresponding quantum dynamics. However, there are exceptions, such as the following:

- i) Spherically symmetric wave-packets $\psi(r, t)$.
- ii) Wave-packets of the kind $\psi(\mathbf{r}, t) = \sum_k \alpha_k f_k(\mathbf{r}) e^{iE_k t}$ where $\alpha_k, f_k \in \mathbb{R}$, and the energies E_k are commensurate
- iii) Stationary wave-packets $\varphi(x, y, z) e^{-iEt}$, where $\varphi(x, y, z) = \varphi^*(x, -y, z)$. For example, $\psi(r, \theta, \phi, t) = e^{iEt} \sum_k \alpha_k f_k(r, \theta) e^{im_k \phi}$, where $\alpha_k, f_k \in \mathbb{R}$, $m_k = 0, \pm 1, \dots$

The wave-packets i), ii) always give rise to regular QFs, whereas the wave-packet iii) only in some situations. Although the explanation of these facts is not very difficult, it cannot be given in few words, and it will be shown within a more general framework elsewhere. Here, we confine ourselves to note that iii) includes, in particular, the stationary solutions $R_{nl}(r) Y_{lm}(\theta, \phi) e^{-iE_n t}$ of the time-dependent Schrödinger equation for the hydrogen atom. In this latter case, all orbits are circles centred on the z -axis and parallel to the (x, y) -plane. Obviously the corresponding Λ_1 is zero.

Fig. 6 shows the check of the relationship (24). Although this relationship holds, in principle, for any $t > 0$, in practice, its validity is restricted to a finite time interval $0 < t < T$, where T depends on the numerical accuracy. In our case T is very large (of order 10^6 a.u.). In Fig. 6, to put in evidence discrepancies in a short time interval, we have reduced the accuracy in the calculation of the LEs.

Fig. 7 illustrates that

$$\lim_{t \rightarrow +\infty} \sum_{i=1}^3 \lambda_i(t, \mathbf{r}(0)) = 0, \quad \forall \mathbf{r}(0) \in \mathcal{R}. \quad (32)$$

In virtue of the relationship (24), limit (32) means that our trajectories do not reach the nodes of the wave-packet (27) and that the density $\rho(\mathbf{r}(t), t)$ keeps bounded. Actually (see Fig. 6), the density $\rho(\mathbf{r}(t), t)$ along a given trajectory

shows bounded oscillations. Thus, recalling Property 2, we can also say that our QF, as concerns the variation of the size of volume elements, has not any definite character, but it is expected to be conservative on average. We have employed systematically the limit relationship (32) to check the accuracy of the LE calculation.

Finally, Fig. 8 illustrates the fact that the pattern of a chaotic QF is very sensitive to tiny modifications in L^2 -norm of the initial conditions in the IVP (8). To give a clear idea of this phenomenon, Fig. 8 displays only the components $z(t)$ (as functions of t) of the points pursuing two typical chaotic trajectories, both starting at $t = 0$ from the same initial point, but pertaining to two different QFs. The first QF is relative to the IVP (8) with initial condition $\psi_0(\mathbf{r})$, obtained by setting $t = 0$ in (27). The second QF is relative to the IVP (8) with initial condition $\psi'_0(\mathbf{r})$, obtained from $\psi_0(\mathbf{r})$ by a tiny modification of the coefficients of the corresponding linear combination, such that $\|\psi_0 - \psi'_0\| = 10^{-4}$.

SPIN CONTRIBUTIONS FOR THE QLE

When we deal with a spinning particle —as is the electron of the hydrogen atom— we must take into account also the presence of the intrinsic angular momentum. The presence of the spin in the Schrödinger theory does not affect the stationary energy levels and the wave-equation to be used is, as usual, Eq. (2). Nevertheless, we have to consider the spin, not only to obtain the allowed stationary states of atoms (because of the Pauli principle and the “exchange interaction”), but also to write the *complete* expression of the conserved probability current for the Schrödinger equation. The complete Schrödinger current can be got [18, 19, 20, 21]: a) taking the non-relativistic limit of the Dirac current; b) considering the Pauli current in the particular case of a spin-eigenstate wave-function; c) directly from the Schrödinger equation, by considering the privileged direction which the spin introduces in the space. Let us remember that any solution of the Schrödinger equation is always a spin eigenstate along some space direction, because the Hamiltonian $-\hbar^2 \Delta/2m + U$ does not contain any spin term. Then the “complete” form for Schrödinger wave-function for a spinning particle actually is $\sqrt{\rho} e^{iS/\hbar} \chi$ where χ is a *constant* 2-components Pauli spinor. Following Landau [18] we can write the conserved Schrödinger current as follows:

$$\mathbf{j} = \frac{\rho}{m} \nabla S + \frac{\hbar}{2m} \nabla \rho \times \mathbf{s}. \quad (33)$$

where \mathbf{s} is the constant unit versor in the direction of the spin: $\mathbf{s} \equiv \chi^\dagger \boldsymbol{\sigma} \chi / \chi^\dagger \chi$, $\boldsymbol{\sigma}$ being the usual Pauli 2×2 vector matrix. [38] When the polarization direction is chosen parallel to the z -axis, i.e., $\mathbf{s} = (0; 0; s_z)$, $s_z = \pm 1$, we have for the spin-part of the current:

$$\frac{\hbar}{2m} \nabla \rho \times \mathbf{s} = s_z (\nabla_y \rho; -\nabla_x \rho; 0). \quad (34)$$

The current in Eq. (33) appears as a sum of the translational, “newtonian”, part $\rho \nabla S / m$ which, at the classical limit ($\hbar \rightarrow 0$), is parallel to the classical impulse (equal to \hbar times the gradient of the action); and of a “non-newtonian”, rotational part due to the spin, $\nabla \rho \times \mathbf{s} / 2m$, which vanishes only at the classical limit, i.e. for spinless bodies, *but not in the non-relativistic limit*, i.e. for a small momentum \mathbf{p} . Let us stress that for *any solution of the Schrödinger equation the spin part of the current is conserved* because the curl of a divergence identically vanishes:

$$\nabla \cdot [\nabla \rho \times \mathbf{s}] = \nabla \cdot [\nabla \times (\rho \mathbf{s})] = 0;$$

as a consequence, if $\rho \nabla S / m$ is conserved, quantity $\rho \nabla S / m + \hbar \nabla \times (\rho \mathbf{s}) / 2m$ is conserved as well:

$$\partial_t \rho + \nabla \cdot \left(\frac{\rho}{m} \nabla S \right) = \partial_t \rho + \nabla \cdot \left(\frac{\rho}{m} \nabla S + \frac{\hbar}{2m} \nabla \rho \times \mathbf{s} \right) = 0.$$

Let us also remark that *the spin part of the conserved current results to be of the same order of the scalar-newtonian term*; actually, in the case of *real* wave-functions, the spin part is the non-vanishing one in the probability current. [39] Let us finally recall that also in Bohm Mechanics the inclusion of the spin part in the non-relativistic velocity field is requested for spinning systems [4, 22]. For a n -particles system Eq. (4) generalizes as follows in the presence of spin:

$$\mathbf{j}_i(\mathbf{r}, t) := \frac{\rho(\mathbf{r}, t)}{m_i} \nabla_i S(\mathbf{r}, t) + \frac{\hbar}{2m_i} \nabla_i \rho(\mathbf{r}, t) \times \mathbf{s}_i. \quad (35)$$

while the velocity field $\mathbf{j}_i(\mathbf{r}, t) / \rho$, which for a spinless particle consists of the only term $\nabla_i S(\mathbf{r}, t) / m_i$, now becomes

$$\mathbf{v}_i(\mathbf{r}, t) := \frac{1}{m_i} \nabla_i S(\mathbf{r}, t) + \frac{\hbar}{2m_i \rho(\mathbf{r}, t)} \nabla_i \rho(\mathbf{r}, t) \times \mathbf{s}_i. \quad (36)$$

As it is easy to check, all the properties of the QF proved in Sec. 3 still equally hold in the presence of spin. We have performed several numerical calculations of the chaotic quantities for the hydrogen atom considering the spin: that is, by integrating the above “complete” velocity field. We get results quite similar to the ones obtained in the absence of spin and discussed in the previous section, but the spin part of the quantum flow seems to increase slightly the chaos with respect to the spinless case. As an example, for the wave-packet

$$\psi(\mathbf{r}, t) = \frac{1}{\sqrt{3}} (\varphi_{100}(\mathbf{r}) e^{\frac{i}{\hbar} t} + \varphi_{210}(\mathbf{r}) e^{\frac{i}{\hbar} t} + \varphi_{211}(\mathbf{r}) e^{\frac{i}{\hbar} t}), \quad (37)$$

with spin projection $s_z = +1$, we have obtained (after four runs, varying the accuracy parameters, etc.) the following value for the QLE: $\Lambda_1 = 1.022 \cdot 10^{-2}$.

CONCLUDING REMARKS

In this paper, we have proposed a precise definition of chaos in quantum dynamics. This definition is based only on basic concepts and tools of the theory of chaos in dynamical systems and, contrarily to previous papers, it does not require any new interpretation of quantum mechanics. The characterization of chaos in quantum dynamics introduced by us may be looked upon, in a sense, as the direct analogue of classical chaos and thus, it attempts to reduce the gap between classical chaos and quantum chaos according to the definition in most current literature. The present work stimulates further investigations mainly on two fundamental problems. The first one concerns the correlation with classical chaos. We expect that, if we adopt the criterion for the classical limit described in Ref. [4], quantum chaos here introduced matches with classical chaos. The other problem is that of seeing if the values of the QLEs may be related to observable quantal quantities. We want to investigate these two problems in a next paper and work in this direction is already in progress.

The authors would like to thank G.G.N. Angilella, M. Baldo, M. Baranger, S.P. Goldman, V. Latora, F. Raciti, A. Rapisarda and E. Recami for many helpful discussions. This work has been supported by INFN, Sezione di Catania, and by MURST.

- [1] R. V. Jensen, *Nature* **355**, 311 (1992).
- [2] R.C. Hilborn, *Chaos and non linear dynamics* (Oxford Univ. Press, New York, 1994).
- [3] M. Reed and B. Simon, *Methods of modern mathematical physics* (Acad. Press, New York, 1972), Vol I; (Acad. Press, New York, 1975), Vol II; T. Kato, *Perturbation theory for linear operators* (Springer, Berlin, 1966).
- [4] P. R. Holland, *The quantum theory of motion* (Cambridge University Press, Cambridge, 1993).
- [5] R. H. Parmenter and R. W. Valentine, *Phys. Lett. A* **201**, 1 (1995).
- [6] U. Schwenghelbeck and F. H. M. Faisal, *Phys. Lett. A* **207**, 31 (1995); G. Iacomelli and M. Pettini, *Phys. Lett. A* **212**, 29 (1996); S. Sengupta and P. K. Chattaraj, *Phys. Lett. A* **215**, 119 (1996).
- [7] V. I. Arnold, *Equazioni differenziali ordinarie*, (Ed. Mir, Moscow, 1979).
- [8] R. M. M. Mattheij and J. Molenaar, *Ordinary differential equations in theory and practice* (John Wiley & Sons, Chichester, 1996).
- [9] K. Berndl, D. Dürr, S. Goldstein, G. Peruzzi, and N. Zanghi, *Comm. Math. Phys.* **173**, 647 (1995).
- [10] F. Scheck, *Mechanics* (Springer, Berlin, 1994).
- [11] J. L. Mc Cauley *Classical mechanics* (Cambridge Univ. Press, Cambridge, 1997).
- [12] G. Benettin, L. Galgani, A. Giorgilli, and J.-M. Strelcyn, *Meccanica* **15**, 9 (1980).
- [13] J. P. Eckman and D. Ruelle, *Rev. Mod. Phys.* **57**, 617 (1985).
- [14] K. E. Atkinson, *An introduction to numerical analysis* (John Wiley & Sons, New York, 1989); K. Geist, U. Parlitz and W. Lauterborn, *Prog. Theor. Phys.* **83** 875 (1990).
- [15] G. Benettin, L. Galgani, A. Giorgilli, and J.-M. Strelcyn, *Phys. Rev. A* **14**, 2338 (1976).
- [16] T. S. Parker and L. O. Chua, *Practical numerical algorithms for chaotic systems* (Springer, New York, 1989).
- [17] G. Benettin, L. Galgani, A. Giorgilli, and J.-M. Strelcyn, *Meccanica* **15**, 21 (1980).
- [18] L.D. Landau and E.M. Lifshitz, *Meccanica quantistica - Teoria non-relativistica*, p.553 (Editori Riuniti - Edizioni MIR; Roma, 1978)
- [19] D. Hestenes: *Space-time algebra* (Gordon & Breach; New York, 1966); *New foundations for classical mechanics* (Kluwer; Dordrecht, 1986); *Found. Phys.* **20**, 1213 (1990); **23**, 365 (1993); **15**, 63 (1985); **12**, 153 (1981); *Am. J. Phys.* **47**, 399 (1979); **39**, 1028 (1971); **39**, 1013 (1971); *J. Math. Phys.* **14**, 893 (1973); **16**, 573 (1975); **16**, 556 (1975); **8**, 798 (1979); **8**, 809 (1967) 809; **8**, 1046 (1967); D. Hestenes and A. Weingartshofer (eds.), *The electron* (Kluwer; Dordrecht, 1991)
- [20] G. Salesi, *Mod. Phys. Lett. A* **11**, 1815 (1996); G. Salesi and E. Recami, *Found. Phys. Lett.* **10**, 533 (1997); G. Salesi and E. Recami, *Found. Phys.* **28**, 763 (1998); E. Recami and G. Salesi, *Phys. Rev. A* **57**, (1998) 98, and refs. therein

- [21] S. Esposito, Found. Phys. Lett. **12**, 167 (1999)
- [22] E. Deotto and G.C. Ghirardi, Found. Phys. **28**, 1 (1998)
- [23] L. de Broglie: C.R.Acad.Sc.(Paris), **183**, 447 (1926); *Non-Linear Wave Mechanics* (Elsevier; Amsterdam, 1960); *Théorie Générale des Particules à Spin* (Gauthier-Villars; Paris, 1954)
- [24] In the present paper we prefer the latter denomination.
- [25] According to this picture, the point \mathbf{r} when it varies on $\mathcal{P}(t)$ will be denoted by $\mathbf{r}(t)$. The volume element $d\mathbf{r}$ on $\mathcal{P}(t)$ will be denoted by $d\mathbf{r}(t)$.
- [26] In what follows, we set $t_1 = 0$. Thus $\mathbf{r}_1 = \mathbf{r}_0$. To simplify notation, we shall write $\Phi(t, \mathbf{r}_0), \Phi(\cdot, \mathbf{r}_0)$ etc., for $\Phi(t, 0, \mathbf{r}_0), \Phi(\cdot, 0, \mathbf{r}_0)$ etc., respectively.
- [27] In what follows, we denote by $\psi(\mathbf{r}, t)$ the solution of the IVP (8) which gives rise to the QF considered.
- [28] Throughout this paper *volume element* means a volume small enough, in principle infinitesimal.
- [29] The Jacobian depends also on the initial time $t = 0$. But according to footnote 3, we have written $J(t, \mathbf{r}_0)$ instead of $J(t, 0, \mathbf{r}_0)$.
- [30] All the quantities introduced above, $\lambda_i(\mathbf{r}_0), \lambda_i(t, \mathbf{r}_0), U_{\mathbf{r}_0}(t)$, etc., depend on the initial time $t = 0$. But according to footnote 3, we have not displayed 0.
- [31] Henceforth, we shall denote the QLEs by Λ_i instead of $\Lambda_i(0)$.
- [32] In this section, we call such a solution simply *wave-packet*.
- [33] Throughout this section, atomic units (a.u.) are employed.
- [34] The point \mathbf{r}_0 denotes the starting point of each trajectory. We do not need to specify this point, which, obviously, varies with the trajectory.
- [35] The accuracy parameters changing in the four different runs, are some parameters which rule the numerical accuracy of the employed NAG algorithms as the integration procedure of the IVP (9) or the numerical squaring. After changing those parameters the computed trajectories can vary a lot because of the presence of chaos. Notwithstanding the global QLE, coming out from the integration over the whole domain \mathcal{R} , is not sensitively influenced by the variation of the accuracy parameters (the change in the QLEs results to be less than 10%).
- [36] The lower endpoint of the interval is chosen equal to $0.4t_i$ because we have no interest in studying the behavior of λ_1 at small time; we will instead establish if λ_1 converges to 0 or not, that is, if the trajectory is regular or not.
- [37] The “fixed threshold” was estimated through an empirical, cut-and-try procedure and results to be of the order of the typical asymptotic value (very close to 0 at sufficiently large times) of λ_1 found for trajectories known to be regular.
- [38] Let us incidently remark that, by contrast with the Schrödinger-case, the most general wave-function solution of the Pauli equation must be written in the non-decomposed form $\chi(\mathbf{r}, t)$, where the two spinor components vary in space and in time independently each other. This happens since the spin is not anylonger conserved, e.g. because of its coupling $-e\mathbf{s} \cdot \mathbf{H}/2m$ with some external magnetic field. Respect to the Schrödinger-case, the spin term in the conserved current cannot be anylonger written as $\nabla \rho \times \mathbf{s}/2m$ but only as $\nabla \times [\chi(\mathbf{r}, t)^\dagger \boldsymbol{\sigma} \chi(\mathbf{r}, t)]/2m$ [18, 20].
- [39] As is known, the eigenfunctions corresponding to non-degenerate energy eigenvalues are always real: in fact, the phase S is uniform and equal to a constant (which, for the “global phase gauge invariance”, may be assumed equal to zero). We refer ourselves to the $l = 0, n \geq 1$ stationary states of a particle inside a well (or a box) and of the hydrogen atom, as well as to the $m = 0, n \geq 0$ stationary states of a particle in a uniform magnetic field. Even for some systems with degenerate energy levels, as, for instance, the spherical harmonic oscillator, the eigenfunctions are real. For real wave-functions, neglecting the spin, we should have $\mathbf{j} = \nabla S = 0$ everywhere. As it was first remarked by Einstein and Perrin and by de Broglie, [23] such a result seems to be in contrast, from a classical point of view, with the non-vanishing of the energy eigenvalue for those stationary states. But if we consider the spin component of the current —which depends on the gradient of ρ , and not on the gradient of the phase— we have a rotational motion around the spin polarization direction, and the quantum “zero-point” energy arises as a kinetic-like energy.

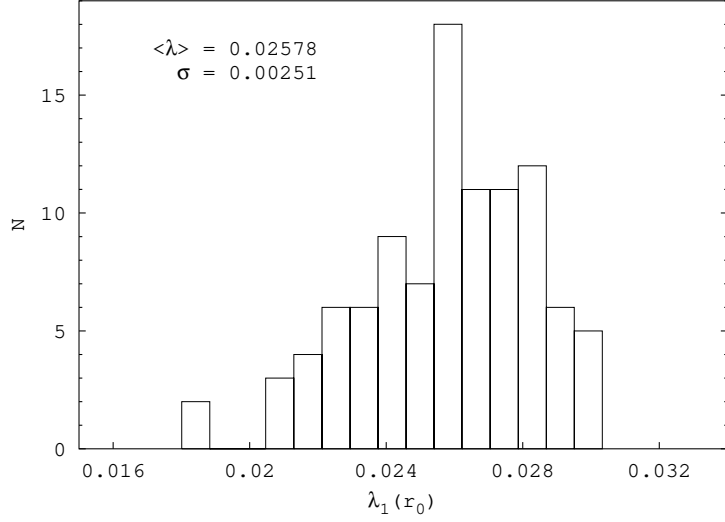


FIG. 1: Histogram relative to the distribution of the values found for $\lambda_1(r_0)$ over 100 trajectories, all starting from the same initial point r_0 but evaluated with slightly different accuracy. N is the number of trajectories, $\langle \lambda \rangle$ is the expectation value and σ is the standard deviation.

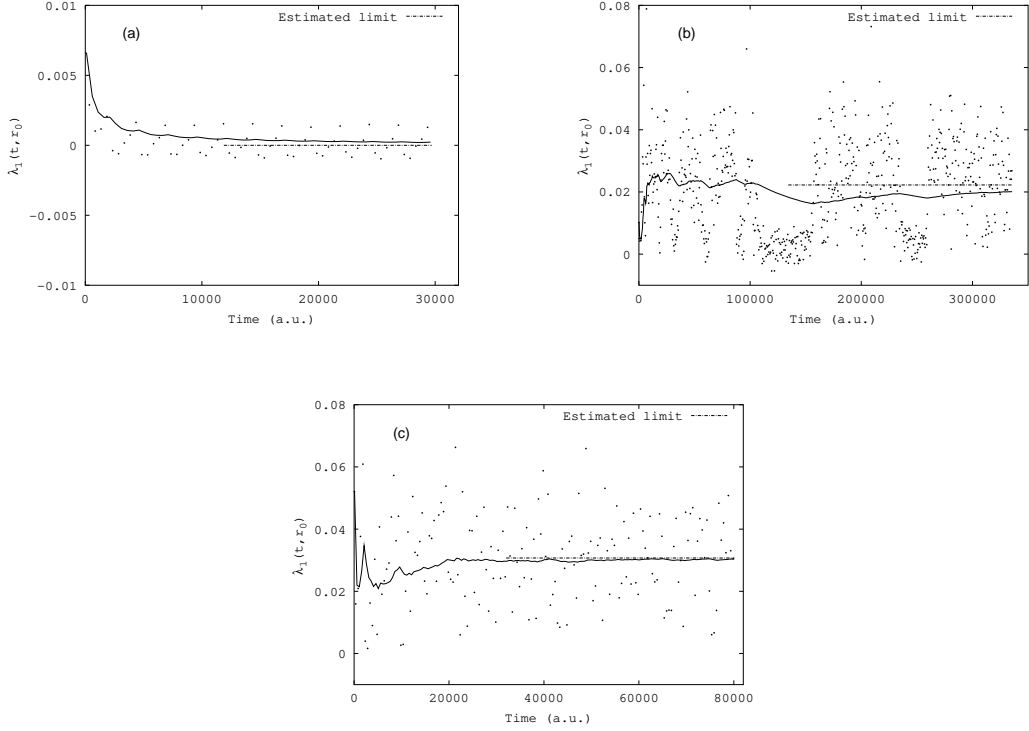


FIG. 2: Figures (a)-(c) are relative, respectively, to a typical (regular, “intermittent” chaotic, chaotic) trajectory. The solid curve represents the LE $\lambda_1(t, r_0)$ as function of t and the dots represent quantities (29).

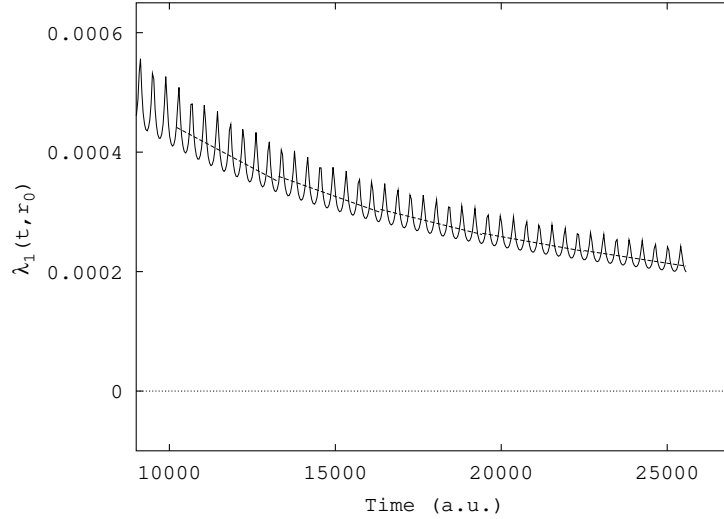


FIG. 3: Convergence criterion for a typical regular trajectory starting from \mathbf{r}_0 . The solid curve represents the LE $\lambda_1(t, \mathbf{r}_0)$ as a function of t . The dashed straight lines represent the LLSAs.

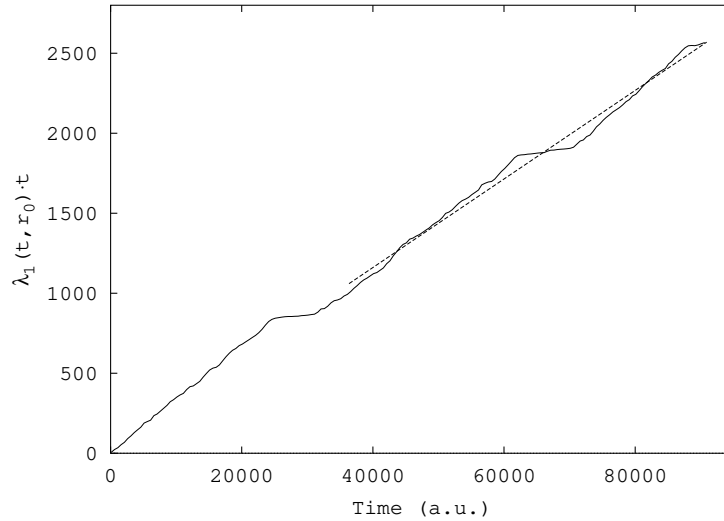


FIG. 4: Convergence criterion for a typical chaotic trajectory starting from \mathbf{r}_0 . The solid curve represents $\lambda_1(t, \mathbf{r}_0)t$ as a function of t . The dashed straight line represent the LLSA.

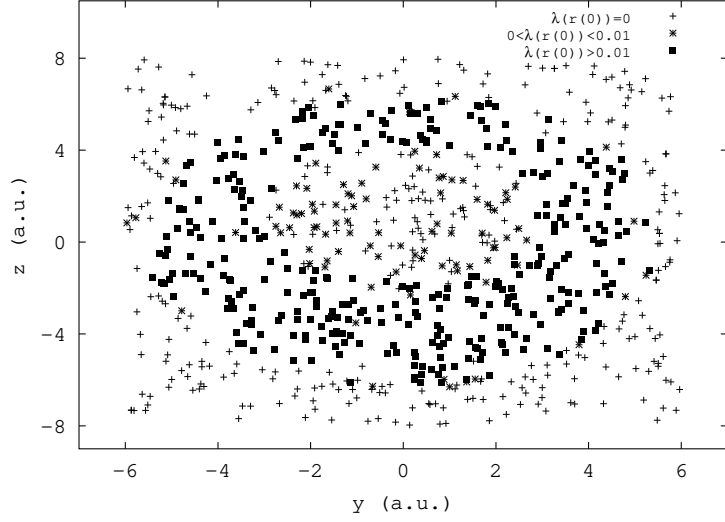


FIG. 5: Projection onto the (y, z) -plane of all the initial conditions in the region $\{(x, y, z) \in \mathcal{R} : -0.5 < x < 0.5\}$ and relative to the trajectories evaluated in the four runs to calculate Λ_1 . Three regions of different degree of chaos are put in evidence.

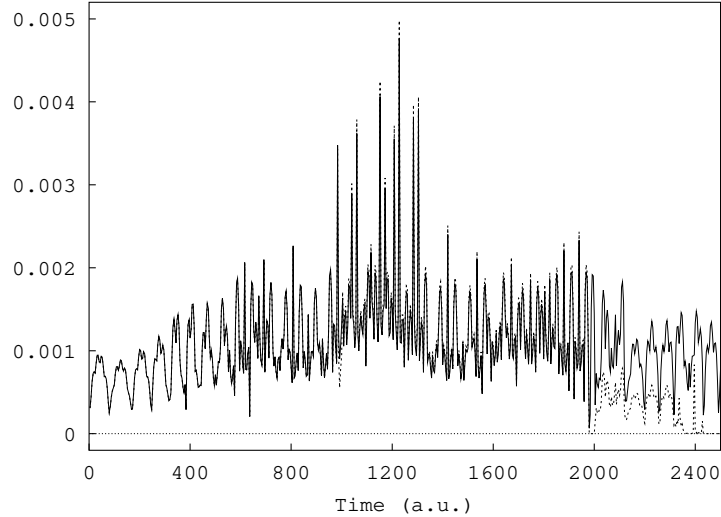


FIG. 6: Check of Eq. (24). The solid curve represents the probability density $\rho(\mathbf{r}(t), t)$ as given by the wave-packet (27) along a typical chaotic trajectory. The dashed curve represents $\rho(\mathbf{r}(t), t)$ along the same trajectory but evaluated through (24).

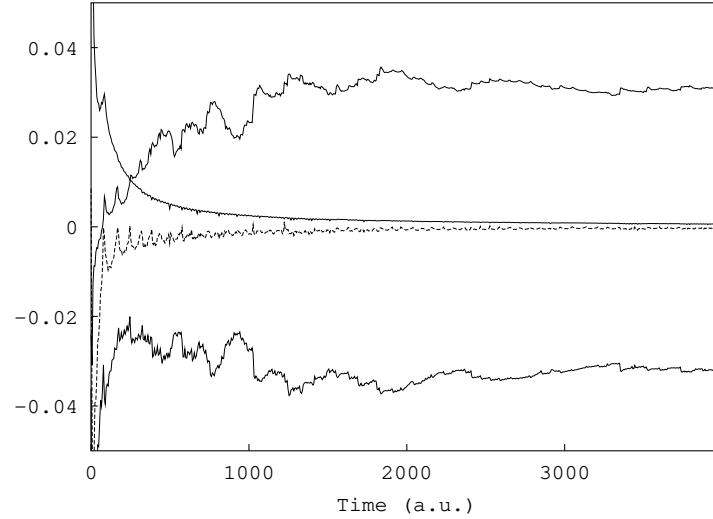


FIG. 7: Check of the limit relationship (32). The solid curves represent the three LEs: $\lambda_1(t, \mathbf{r}_0), \lambda_2(t, \mathbf{r}_0), \lambda_3(t, \mathbf{r}_0)$ as functions of t , of a typical chaotic trajectory starting from \mathbf{r}_0 . The dashed curve represents $\sum_{i=1}^3 \lambda_i(t, \mathbf{r}_0)$.

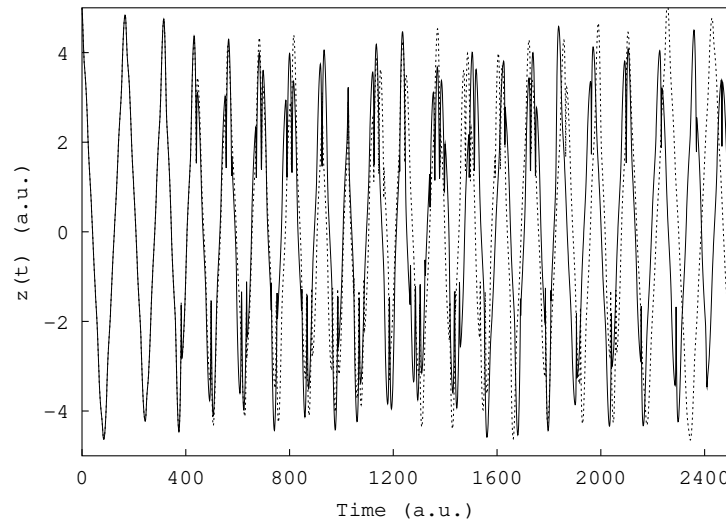


FIG. 8: Dependence of the QF pattern on the initial condition in the IVP (8).